Environment, Development and Sustainability
https://doi.org/10.1007/s10668-024-05304-y

Enhancing solar still performance with hybrid nanofluid: a comprehensive assessment of energy, exergy, economics, and environmental impact using a novel fractional model

E. F. El-Gazar[1] · Mohamed S. Yousef[2] · Abdelrahman M. Elshaer[3] · Mahmoud A. Khattab[1] · T. A. Mouneer[3] · A. A. Hawwash[3]

Received: 23 August 2023 / Accepted: 5 August 2024

Abstract
In the present study, the thermal performance of a modified solar still (MSS) system coupled with hybrid nanofluid (HNF) of titanium oxide (TiO_2) and silicon oxide (SiO_2) has been investigated theoretically based on energetic, exergetic, economic, and enviroeconomic assessment. The model of the MSS has been introduced using a new numerical technique of the Atangana-Baleanu fractional derivative. The fractional model of the MSS system is presented under various weather circumstances (winter and summer seasons) in Egypt to show the impact of HNF on the MSS output: temperatures, freshwater productivity, exergy, and energy efficiencies. The outcomes of the fractional model are contrasted to those derived from actual experimental data collected under varying climatic conditions in Upper Egypt. Numerical findings demonstrate specific consistency between the experimental results and the proposed model of the solar still (SS), with a percentage of error of 4.65% in freshwater productivity. Moreover, using hybrid nano enhances daily productivity in the summertime by 27.2% and in the wintertime by 21.7%, increasing efficiencies. Additionally, a comparative economic and environmental assessment has been investigated for all the proposed desalination systems without and with HNF. The findings found that the cost per liter of MSS was 44% lower than that of the conventional solar still (CSS) during the summer season. Using exergy and energy approaches, MSS reduced CO_2 by 22% and 29.6% more during the winter.

Keywords Atangana-Baleanu · Fractional differential equation · Solar still · Hybrid nanoparticles · Economical assessment · Environmental assessment

Abbreviations
AB Atangana- Baleanu

✉ E. F. El-Gazar
eman.elgazar@ejust.edu.eg

1 Basic Science Department, Benha Faculty of Engineering, Benha University, Benha, Egypt

2 Department of Thermal and Fluid Engineering, Universidad Carlos III de Madrid, Av. de La Universidad, 30, 28911 Leganés, Madrid, Spain

3 Mechanical Engineering Department, Faculty of Engineering, Benha University, Benha, Egypt

Published online: 24 August 2024

AMC	Annual Maintenance Cost
ASV	Annual Salvage Value
CPL	Cost Per Liter
CSS	Conventional Solar Still
CRF	Capital Recovery Factor
HNF	Hybrid Nanofluid
MSS	Modified Solar Still
SSF	Sinking Fund Factor
UAC	Total Annual Cost

List of symbols

A	Area in m^2
C	Specific heat in J/kg.K
G	Solar irradiance in W/m^2
h	Heat transfer coefficient in $W/m^2.K$
H	Evaporation coefficient of heat transfer
k	Thermal conductivity W/m.K
m	Mass in Kg
P	Capital Cost in $
T	Temperature in °C
t	Time in second
v	Wind velocity in m/s

Greek symbols

η	Efficiency
Φ	Volume fractional
ρ	Density in kg/m^3
μ	Viscosity
α	Order of fractional derivative ($0 < \alpha \leq 1$)
ƛ	The latent heat of vaporization

Subscripts

ab	Absorber Plate
amb	Ambient
exe	Exergy
cw	Convection
ew	Evaporation
eff	Effective
hn	Hybrid Nanofluid
gl	Glass
rw	Radiation
th	Thermal
wat	Water

1 Introduction and literature review

In recent years, access to clean, healthy, and pure water is indeed one of the most critical issues facing humanity. Without adequate access to safe water, communities face numerous challenges related to health, sanitation, food security, and economic development.

Approximately 97% of Earth's water is saline, found in oceans and seas, while only about 3% is freshwater. This freshwater exists in various forms, including surface water such as rivers, lakes, and freshwater wetlands, as well as groundwater and frozen water in polar ice caps, glaciers, and snowfields (Abujazar et al., 2016; Bait & Si-Ameur, 2018; Rashidi et al., 2016).

By 2035, over a quarter of the people on our planet will be affected by water scarcity due to the growth in the world's population and the increasing query for water consumption. As a result, desalination technology is regarded as one of the most significant processes for obtaining potable freshwater depending on exploiting the sources of brackish water (seas and oceans). However, most of the desalination technologies that have been developed recently have complex structures and designs. Additionally, most of these desalination systems rely on fossil fuel sources, meaning their operating and maintenance costs will continue to rise dramatically due to the limited resources for fossil fuels. Energy storage materials could used as a source of heat inside the SS during the night (Hawwash et al., 2023; Hawwash et al., Sep. 2019). The SS is a simple and economical design for producing clean water, which depends on the incident solar radiation to convert salty impure water into filtered water (El-Gazar et al., 2020).

Hussen et al. (2023) investigated four distinct designs of the SSs. The tested SS systems were conventional, pyramid, double slope, and tubular SS. For mitigating the effect of shadow inside the double slope SS and pyramid SS leading to a rise inside the water basin. In addition, Phase Change Materials (PCM) were employed to enhance thermal storage performance. The design of pyramid SS with PCM showed the greatest values of 116.4%/51.3%, for productivity and thermal efficiency, respectively. Aly et al. (2023) enhanced the output of tabular SS by presenting a new design, the oval tubular SS coupled with PCM and cover plate cooling. The productivity and efficiency of the oval tubular SS were enhanced by 32.42% and 41.26%, respectively.

Alshqirate et al. (2023) improved the freshwater productivity of conventional SS with natural Palmately leaf fibers. The outcomes found that the daily total freshwater yield was 5160.8 gm/m^2 by using natural fiber, with an increasing percentage of 44.5% relative to the CSS. Manoj Kumar et al. (2022) conducted an experiment investigating the effect of thermal energy storage/ SS integration. Inorganic PCM and nano-doped PCM were integrated with a single-sloped conventional SS. The findings showed that using inorganic PCM and nano/PCM composite boosted the percentage of freshwater yield from the SS by 26.63% and 45.23%, respectively. Hameed et al. (2022) evaluated the thermal performance of single slope SS integrated with fins of a square area involved in the absorber plate. The work also studied the efficacy of SS glass cover cooling methodology. The findings reported an improvement in the water productivity of the SS/fins combination by 40%. Also, the study reported a significant improvement in productivity with cover cooling.

Ahmed et al. (2022) investigated the influence of cotton wick material integrating with tubular SS and parabolic concentrator systems. The results revealed that the cotton wick enhanced the setup efficiency and productivity by 24.45% and 29.11%, respectively. Angappan et al. (2023) studied the integration of SS and box-shaped solar cookers to boost SS water productivity. The outcomes reported that the conventional and modified SS daily productivities reached nearly 4 L/m^2 and 6 L/m^2, respectively, with an increasing percentage of 41% compared to the conventional one. Chauhan et al. (2023) improved the SS output by surface coating of Lauric acid and phosphorus quantum dot material. Two designs of SSs were adopted, the conventional SS and prism-shaped SS. The results showed that traditional and prism-shaped SS with PCM and black coating yielded about 3050 ml/m^2 and 3600 ml/m^2, respectively.

Abdullah et al. (2023) modified a single slope SS by integrating Nano- PCM, with an external condenser, copper water heating coil, internal, and external reflectors to enhance freshwater productivity. Combining external reflectors (top and bottom) with external condenser, and PCM improved the SS productivity by about 42%, 57%, and 41%, respectively. Kumaravel et al. (2022) investigated the performance analysis of a single slope SS integrated with thermal energy storage with blue metal stones and pebble stones. The findings showed that combining the two types of rocks and their integration with the SS increased productivity by 18% relative to conventional SS.

Much research was dedicated to enhancing SS's thermal and productivity performance by adopting numerical and mathematical models. Moustafa et al. (2022) increased the tubular SS's water productivity and energy efficiency by attaching an electric heater to the still basin powered by a solar photovoltaic (PV) panel (El-Gazar et al., 2023a). Also, the work developed a model based on artificial intelligence (AI) for predicting the SS's water yield and thermal efficiency. The findings revealed that the modified SS had an average daily accumulated water productivity of nearly 3 L/m^2 with a 31.85% enhancement percentage. Mittal (2021) delivered a Computational Fluid Dynamics (CFD) modeling of a single slope SS using ANSY S Fluent. The CFD model approach computationally proved its effectiveness in capturing the distillate water output at various configurations, provided that the bottom and top surface temperatures are identified. Mohsenzadeh et al. (2022) established and validated a transient model experimentally to investigate a passive SS. The evaporation chamber was designed with different aspect ratios, and all the cases were investigated. The study revealed that the aspect ratio of the SS evaporation chamber increased and produced more fresh water.

Lisboa et al. (2022) performed a model analysis for the freshwater productivity enhancement techniques of SSs. The study concluded that the dominant factors that enhance water productivity were structure design, water depth, basin-glass temperature difference, insulation, and solar irradiation. Keshtkar et al. (2020) introduced a CFD mathematical model to study the impact of different design factors of passive basin SS. The findings show that the SS freshwater yield increased by about 14% when the wind velocity was raised by 5 m/s. The SS productivity also increased by 3.5% when the glass width decreased to 2 mm. Hassan et al. (2022) provided a novel simulation model for estimating SS's performance. The model results were proven experimentally, and different materials of SS walls were studied. The water productivity per unit area of the basin was about 2 and 4 kg/m^2 for glass and wooden walls, respectively. A numerical simulation was modeled by Gupta et al. (2022) to investigate the performance of a single slope SS under different climate conditions in India. The model accurately predicted the SS's performance at distinct conditions.

Nanofluids were used to increase the SS efficiency in more studies (Ajit et al., 2023; Chen et al., 2023; Mustafa et al., 2023; Sahu & Tiwari, 2024). Kabeel et al. (2019) investigated experimentally a new absorber plate of a pyramid SS covered with titanium oxide nanoparticles black coating. The findings summarized that water yield was increased by the decrease in the water depth. The coated absorber plate improved the freshwater yield by 12% at maximum water depth. Rashidi et al. (2018) examined numerically the influence of nanofluid insertion on the freshwater output of a stepped SS. The outcomes showed that raising the nanoparticle percentage by 5% increased the hourly water productivity by about 22%. Sahota et al. (2019) investigated the performance of a double slope SS with alumina and Multi-Wall Carbon Nano Tubes (MWCNTs) water-based nanofluid. The results found a remarkable improvement in SS's evaporative heat transfer coefficient and freshwater output by adopting water-based nanofluids.

Sharshir et al. (2022) conducted an experimental study investigating the performance of pyramid SS integrated with evacuated tubes, nanofluid, external condensers, and ultrasonic foggers. The results showed that modified SS with six evacuated tubes, nanofluid, and an external condenser had increased the freshwater yield, exergy efficiency, and energy efficiency by about 132%, 75%, and 28%, respectively. Alsehli et al. (2022) implemented a new design for SS and improved freshwater productivity by incorporating graphene nanoplatelet/platinum hybrid nanofluid. The study found that mixing the nanoparticle with the base fluid led to a remarkable growth in freshwater productivity.

Mustafa et al. (2023) performed a two-phase analysis on integrating aluminium-based nanofluid in SS. AAluminumnanoparticles were utilized in the SS's basin. The results concluded that solar irradiation dominated the PCM maximum temperature, air temperature, and PCM volume fraction. Maatki et al. (2022) enhanced the heat transfer within a triangular SS using Carbon Nano Tube (CNTs)—based nanofluid. The results showed that the MSS design with nanofluid significantly improved the mass and heat transfer rates. Modi et al. (2022) examined the effect of thermal energy storage materials and nanoparticles on the freshwater productivity of pyramid SS with square shape. The outcome revealed that the SS's total water productivity and efficiency with energy storage were greater by 5% and 5.5%, respectively than nanofluid.

The research adopted hybrid nano-based water for enhancing SS productivity is outlined in the following paragraphs. A fractional modeling technique was adopted by El-Gazar et al. (2021b) to examine the impact of HNF on the performance of a conventional SS. The HNFs adopted were alumina and copper oxide. The results revealed that adopting hybrid nanofluids increased the freshwater's daily productivity by nearly 27% in hot weather conditions and 21% in cold conditions. Shoeibi et al. (2022) numerically evaluated the cover glass cooling of a double-slope SS integrated with HNF (TiO_2-Al_2O_3). The results revealed that the productivity of freshwater improved by 11.09%, compared to the model without a hybrid nanofluid. Rabbi et al. (2021) improved the SS's performance using two-hybrid nanofluids. The freshwater productivity, and efficiency, were 4.99 kg m^{-2} / day, 37.76%, respectively when water was mixed with Al_2O_3–SiO_2 hybrid nanofluid. El-Gazar et al. (2021b) conducted a novel nonlocal model for SS performance investigation integrated with a PV panel, HNF, and saline water preheating. The findings show that the daily SS's productivity was 7.1 kg/m^2 per day when the HNF was employed, leading to an improvement percentage of 10% relative to the SS system without a hybrid nanofluid. Kaviti et al. (2023) studied the water desalination system of a SS using HNF of cerium oxide (CeO_2) nanoparticles and MWCNTs. The modified SS accomplished a high productivity of 1430 mL relative to the CSS, with a peak productivity of 920 mL.

The study of the SS systems did not stop with enhancing the yield and efficiency of the still. Still, it also included work on exergetic analysis, which mainly depends on thermodynamics's second law. Compared to energetic analysis, which relies on the 1st law of thermodynamics, exergy assessment appears to be an effective observation tool for investigating the optimization, performance, thermal design, and evaluation of various energy techniques (Asbik et al., 2016; Gad et al., 2022; Hakim et al., 2018; Ibrahim et al., 2017; Jafarkazemi & Ahmadifard, 2013; Kianifar et al., 2012; Kumar et al., 2020; Ranjan et al., 2016). Indeed, exergy analysis offers valuable insights into the performance of solar still (SS) systems by identifying locations, magnitudes, and types of irreversibilities and losses within the system. Unlike energy analysis, which focuses solely on quantity, exergy analysis considers the quality of energy and provides a more comprehensive understanding of system efficiency. Pal et al. (2018) presented a thermal model for the double slope SS, then studied the exergy and energy assessment for the still system after adding black cotton wicks in the still basin to enhance its efficiency. Another new fractional model for the SS system, which studied the energy and exergy assessment, was presented by El-Gazar et al. (2021a). The fractional model was presented to show the effect of mixing hybrid nanoparticles with salty water on the exergy and energy efficiencies of a SS system coupled with a PV panel. Moreover, Sharshir et al. (2018) compared the conventional SS and the modified still with nanoparticles of copper oxide (CuO) and graphite. The comparison was presented based on evaluating the energetic, energetic, and economic parameters for both the SS with and without using the nanofluid.

Although it is widely acknowledged that the exergy technique may be utilized to represent the performance of SS systems effectively, there are still certain limitations and weaknesses in environmental and economic analyses (Abo-Elfadl et al., 2021; Deniz & Çınar, 2016; Gaur & Tiwari, 2014; Hassan et al., 2020; Joshi & Tiwari, 2018; Singh, 2018; Singh & Tiwari, 2017; Yousef et al., 2022). So, the work on the energy systems has been expanded to include how the desalination system affects the environment and how much -effectiveness it costs. Environmental and economic approaches afford in-depth insight into the cost analysis of the engineering processes and the environmental impact by recognizing the necessary tools in the work conditions. Considering the abovementioned, exergy-economic and environmental approaches are being rapidly applied to evaluate different solar distillations. Among these works, which have been developed recently, was conducted by El-bar et al. (2019), where they studied the (4E) exergy-economic, enviro-economic energy, and exergy, analysis for SS systems integrated with the photovoltaic panel. Based on the environmental approach, the results showed that the conventional still mitigated about 18.99 tons of CO_2 per year, whereas the still coupled PV mitigated 20.89 tons of CO_2.

Yousef and Hassan (2018) studied the performance of a solar distilled system incorporated with energy storage material (PCM) from exergy-environmental and exergy-economic points of view. According to the findings of this study, it was found that the SS system with the PCM material was found to be greener than the conventional still (without PCM). Recently, Fathy et al. (2020) assessed the performance of several configurations of single slope SS with condenser and with forced air cooling based on environmental and economic approaches. Moreover, Lovedeep et al. (2017) analyzed the eco-economic and enviro-economic effects of a solar distillation machine with two basins and several types of nanofluids. The findings showed that there was an increase in annual freshwater yield by 5.2%, 10.4%, and 12% by using CuO, TiO_2, and Al_2O_3 nanofluids, respectively. Additionally, the nanofluid of Al_2O_3 was reported to have a greater enviro-economic parameter than the other varieties of nanoparticles.

More studies enhanced the effectiveness of SS using nanofluids Ravinder et.al (2023) investigated the effect of TiO_2/Jackfruit peel nanofluid with silver balls on the performance of a double-effect solar still. The results presented that the highest efficiency was 20% reached when the energy and exergy were equal 40% and 5.6% respectively, while the depth in water was 0.8 Cm. In another study, a simple stepped solar still was modified three times and investigated experimentally to boost the production rate (Adibi Toosi et al., 2023). The PCM, hybrid nano, and magnetic field were added separately to CSS and examined. It is concluded that the production was increased by 98%, 75%, and 37% by the magnetic field, hybrid nano, and PCM respectively, compared with CSS.

Based on the literature and regarding the author's greatest survey, it has been found that although the main importance of the theoretical works is to improve the performance of solar stills and optimize their working condition, very few mathematical models of solar stills have been presented in comparison to the vast number of experimental works. Moreover, it is discovered that the majority of the given numerical models of desalination systems have been calculated based on classical derivatives, which leads to a large error when compared to the actual experimental results. Furthermore, hybrid nanofluids have demonstrated their ability to improve various solar energy systems. The traditional numerical methods may sometimes struggle to accurately model solar still systems, leading to discrepancies between numerical predictions and actual results. So, the high motivation behind the applied method is to introduce a new nonlocal numerical method based on fractional differential equations to accurately describe the thermal performance of the SS systems and show precise outcomes about its output from water productivity and efficiencies with and without a hybrid nanofluid.

2 The problem statement and the objective of the study

The problem statement of the present study is divided into two significant points: Firstly, the limited availability of mathematical models for solar stills compared to experimental works presents a challenge in optimizing their performance. To overcome this limitation, this research introduces a novel nonlocal (fractional) model based on the Atangana Baleanu fractional derivative. Secondly, due to the lower productivity of the solar still system, hybrid nanoparticles of (Silicon oxide SiO_2 / Titanium Oxide TiO_2) are used with the saline water inside the still basin to enhance its thermal conductivity, and hence increase its output from the fresh water.

The objective of the current research is summarized in three main points as follows:

1. Addressing the Gap in Theoretical Modeling: The limited availability of mathematical models for solar stills compared to experimental works presents a challenge in optimizing their performance. To overcome this limitation, this research introduces a novel nonlocal (fractional) model based on the Atangana Baleanu fractional derivative. By embracing fractional calculus principles, this model is expected to provide more precise predictions and bridge the gap between theoretical simulations and actual experimental outcomes. With an accurate representation of the solar still system's thermal behavior, researchers and practitioners can gain deeper insights into system performance and optimize its design and operation more effectively.
2. Harnessing Hybrid Nanofluids for Enhanced Efficiency: Hybrid nanofluids have shown great promise in enhancing various solar energy systems, making them an attractive avenue for improving solar still performance. By incorporating Silicon Oxide (SiO2) and Titanium Oxide (TiO2) nanoparticles into the briny water, the overall efficiency and productivity of the solar still system can be significantly enhanced. These nanoparticles possess unique heat transfer and energy-absorbing properties, contributing to improved performance metrics. The study meticulously explores the influence of hybrid nanofluids on critical parameters, such as temperatures, freshwater yield, energy efficiency, and

exergy efficiency. By thoroughly analyzing the impact of these novel nanofluid-based systems, this research aims to unlock their full potential in real-world applications.

3. In-Depth Comparative Analysis: The research goes beyond conventional evaluations by conducting a comprehensive comparative analysis encompassing energetic, exergetic, economic, and enviroeconomic parameters. This holistic approach allows for a thorough evaluation of the suggested distilled systems both with and without the implementation of hybrid nanofluids. By considering a wide range of performance metrics, the paper provides a comprehensive assessment of the system's effectiveness, efficiency, economic viability, and environmental impact. This multi-dimensional analysis empowers decision-makers with valuable insights to select the most optimized and sustainable approach for solar desalination.

In the present study, the following points summarized the novelty and contributions of the current work: (i) The suggested fractional (nonlocal) model provides more accurate outcomes and a perfect agreement with the actual data compared to the standard model. (ii) The proportion of inaccuracy between the experimental and theoretical data is reduced by the new non-local model. (iii) hybrid nanoparticles of (Silicon oxide SiO_2/Titanium Oxide TiO_2) have been added to the briny water to enhance the thermophysical characteristics of the conventional fluid and hence raise the solar still's water productivity. (iv) Additionally, the hybrid nanofluid contributes to increasing the traditional SS's exergy and energy efficiencies. (iiv) A comparative study is carried out for all the proposed distillation systems with and without hybrid nanofluid, taking into account energy, exergetic, economic, and enviroeconomic factors.

3 Basic definitions

In this section, various and essential definitions of the fractional operators have been presented as follows (Obembe et al., 2016; Sales Teodoro et al., 2019; Sun et al., 2019; Žecová & Terpák, 2015):

Definition 3.1. The Riemann- Liouville (RL) fractional operator of $T(t)$ is (El-Gazar et al., Oct. 2023b):

$$ {}_{a}^{RL}D_{t}^{\alpha}T(t) = \frac{1}{\Gamma(n-\alpha)} \frac{d^n}{dt^n} \int_a^t (t-\tau)^{n-\alpha-1} T(\tau) d\tau, \quad n-1 < \alpha < n, \tag{1} $$

where $\Gamma(\cdot)$ is the common Gamma function.

Definition 3.2. The Caputo fractional operator of $T(t)$ can be described as.

$$ {}_{a}^{C}D_{t}^{\alpha}T(t) = \frac{1}{\Gamma(n-\alpha)} \int_a^t (t-\tau)^{n-\alpha-1} T^{(n)}(\tau) d\tau, \quad n-1 < \alpha < n, \tag{2} $$

Definition 3.3. The Atangana-Baleanu (AB) Caputo type is.

$$ {}_{0}^{AB}D^{\alpha}T(t) = \frac{M(\alpha)}{1-\alpha}\int_{0}^{t}\dot{T}(\tau)E_{\alpha}\left[-\delta(t-\tau)^{\alpha}\right]d\tau, \quad (3) $$

Where $M(\alpha)$ considers a function satisfied the relation $M(0) = M(1) = 1$.

4 Fractional model

The energy equilibrium formulas for each of the typical SS's three components, a saline water, absorber plate and glass sheet, result in the thermal model represented in Fig. 1. The temperature in each region of the solar still serves as the basis for the energy equilibrium equations for that component. The energy equilibrium formulas can be stated by the presumptions given in (Abujazar et al. 2016; Bait & Si-Ameur, 2018; Rashidi et al., 2016).

4.1 Glass cover equation

The energy emitted from the glass sheet equals the sum of the energy losses. Hence the glass equation can be described by:

$$ G(t)\alpha_{\mathrm{eff},gl}A_{gl} + h_2A_{wat}\left(T_{wat} - T_{gl}\right) = h_{cgl-a}A_{gl}\left(T_{gl} - T_{amb}\right) + h_{rgl-s}A_{gl}\left(T_{gl} - T_{sky}\right) + m_{gl}c_{gl}\left({}_{0}^{AB}\mathbb{D}_{t}^{\alpha}T_{gl}\right), \quad (4) $$

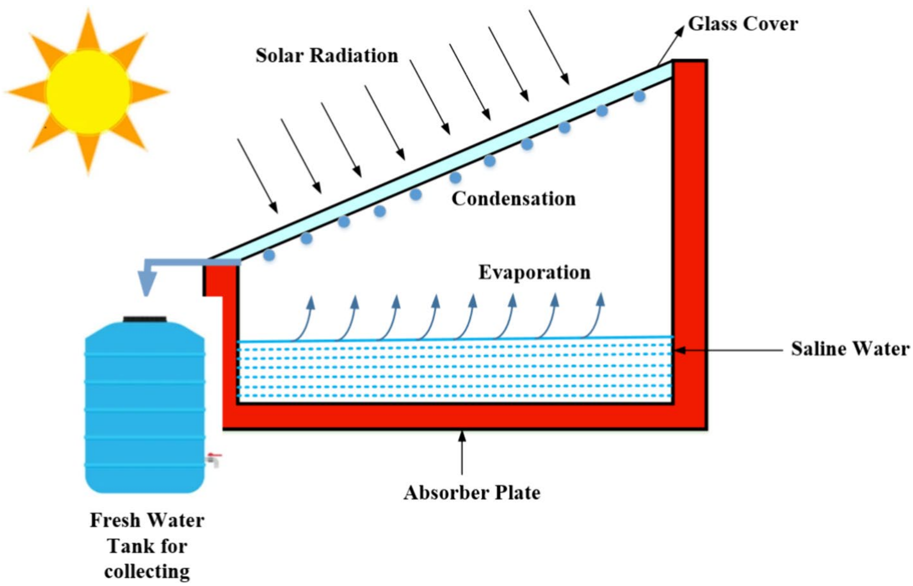

Fig. 1 The Schematic diagram for CSS device

where ${}_{0}^{AB}\mathbb{D}_{t}^{\alpha}$ is the Atangana Baleanu fracrional derivative. The heat transfer coefficients between the atmosphere to the glass are h_{rgl-s} and h_{cgl-a}, respectively, expressed in W/ m^2.K.

$$h_2 = h_{cw-gl} + h_{ew-gl} + h_{rw-gl}, \tag{5}$$

Additionally, the heat transfer coefficients for evaporation, radiation, and convection are h_{cw-gl}, h_{rw-gl}, and h_{ew-gl} in W/m^2.K.

4.2 Salty water equation

The energy from the briny water in the desalination system is comparable to the total amount of energy that the briny water transferred to the glass by convective, radiative, and evaporative coefficients. So, the equilibrium formula for the brackish water can be expressed as:

$$G(t)\alpha_{\text{eff},wat}A_{wat} + h_1 A_{ab}\left(T_{ab} - T_{wat}\right) = h_2 A_{wat}\left(T_{wat} - T_{gl}\right) m_{wat} c_{wat}\left({}_{0}^{AB}\mathbb{D}_{t}^{\alpha} T_{wat}\right), \tag{6}$$

The heat transfer coefficient between the basin and the water is specified by the following equation:

$$h_1 = 0.54\frac{k_{wat}}{x} G_r pr^{0.25}, \tag{7}$$

where G_r, pr are Grashof and Prandtl numbers, respectively.

4.3 Solar still basin equation

The energy released from the basin can be defined as the summation of the energy transferred out by convection heat transfer between the basin and the salted water, energy loss to the air, and energy accumulation inside the SS absorber. This results in:

$$G(t)\alpha_{\text{eff},ab}A_{ab} = h_1 A_{ab}\left(T_{ab} - T_{wat}\right) + H_b A_{ab}\left(T_{ab} - T_{amb}\right) + m_{ab} c_{ab}\left({}_{0}^{AB}\mathbb{D}_{t}^{\alpha} T_{ab}\right), \tag{8}$$

where H_b is the total heat transfer coefficient in W/m^2.K from the absorber plate to the air.

4.4 Output of the solar still

4.4.1 Freshwater yield

The output of the passive distilled system per hour is calculated by:

$$\dot{m}_{ew} = \frac{3600[H_{ew} A_{wat}\left(T_{wat} - T_{gl}\right)]}{\lambda_{fg}}, \tag{9}$$

Where λ_{fg} and H_{ew} are the latent heat and evaporation coefficient of heat transfer between the water and the glass, respectively, and can be assessed by:

$$\lambda_{fg} = 2.4935\left[10^6 - 947.79T_m + 0.13132T_m^2 - 0.0047974T_m^3\right], \tag{10}$$

where $T_m = \frac{T_{wat}+T_{gl}}{2}$.

$$H_{ew} = 0.01623 h_{cw-gl} \left[\frac{P_{wat} - P_{gl}}{T_{wat} - T_{gl}} \right], \tag{11}$$

4.4.2 Energy efficiency

The conventional SS's efficiency is determined as (Abd Elbar et al., 2019; Elbar & Hassan, 2019; Hassan et al., 2019; Yousef et al., 2017)

$$\eta_{th} = \frac{\sum \dot{m}_{ew} \times \lambda_{fg}}{A_{ab} \times \sum G(t) \times 3600}, \tag{12}$$

4.4.3 Exergy efficiency

The exergy analysis employs mass and energy conservation concepts (Abujazar et al., 2016). Exergy efficiency indeed represents the effectiveness of a system in converting input exergy into useful output exergy. It's commonly defined as the ratio of the exergy output of a process or system to the exergy input, expressed as a percentage, as shown in Sharshir et al. (2018); Abo-Elfadl et al., (2021).

$$\eta_{exe} = \frac{E_{X_{out}}}{E_{X_{in}}} = \frac{E_{X_{ew}}}{E_{X_{sun}}}, \tag{13}$$

Where

$$E_{X_{ew}} = H_{ew} A_{wat} \left(T_{wat} - T_{gl} \right) \left(1 - \frac{T_{amb}}{T_{wat}} \right), \tag{14}$$

And.

$$E_{X_{sun}} = A_{gl} G(t) \left[1 - \frac{4}{3} \left(\frac{T_{amb}}{6000} \right) + \frac{1}{3} \left(\frac{T_{amb}}{6000} \right)^4 \right], \tag{15}$$

4.5 Hybrid nano model

Adding nanoparticles with higher thermal conductivity to fluids, for example Titanium Oxide, Silicon oxide, Carbon Nanotubes, and Graphite, is one of the most substantial techniques for improving the heat transfer process (Hawwash et al., 2016, 2018, 2021).

4.5.1 The thermal conductivity

The most popular formula that defines the thermal conductivity for the nanofluid mainly depends on Maxwell–Garnett's model (Hassan & Harmand, 2013; Yang & Jiang, 2017) while in the case of the HNF, the property of conductivity is given by:

$$K_{hn} = \left[\frac{(\emptyset_{\mathrm{SiO2}} K_{\mathrm{SiO2}} + \emptyset_{\mathrm{TiO2}} K_{\mathrm{TiO2}})(1 + 2\emptyset_{hn}) + 2K_{bf}\emptyset_{hf}(1 - \emptyset_{hn})}{(\emptyset_{\mathrm{siO2}} K_{\mathrm{SiO2}} + \emptyset_{\mathrm{TiO2}} K_{\mathrm{TiO2}})(1 - \emptyset_{hn}) + 2K_{bf}\emptyset_{hf}(1 - \emptyset_{hn})} K_{bf} \right], \tag{16}$$

where K_{bf} and K_{hn}, are the thermal conductivities for the base fluid and hybrid nanofluid, respectively, in W/m.K, and $\emptyset_{hn}$ is the volume fraction for hybrid nanofluid such that $\emptyset_{hn} = \emptyset_{\mathrm{SiO2}} + \emptyset_{\mathrm{TiO2}}$.

4.5.2 The density

The density of the nanofluid can be described (Aminossadati & Ghasemi, 2009; Hassan, 2014) by:

$$\rho_{hn} = \left(1 - \emptyset_{hn}\right)\rho_{bf} + \emptyset_{SiO2}\rho_{\mathrm{SiO2}} + \emptyset_{\mathrm{TiO2}}\rho_{\mathrm{TiO2}}, \tag{17}$$

where ρ_{hn} describes the density of hybrid nanofluid, ρ_{SiO2}, and ρ_{TiO2} are densities for the Silicon oxide and the Titanium oxide, respectively, in kg/m^3.

4.5.3 The specific heat

The specific heat of the hybrid nanoparticles (Bourantas & Loukopoulos, 2014) is presented by**:**

$$\left(C_p\right)_{hn} = \frac{\left(1 - \emptyset_{hn}\right)\left(\rho C_p\right)_{bf} + \emptyset_{\mathrm{SiO2}}\left(\rho C_p\right)_{\mathrm{SiO2}} + \emptyset_{\mathrm{TiO2}}\left(\rho C_p\right)_{\mathrm{TiO2}}}{\rho_{hn}}. \tag{18}$$

where $\left(C_p\right)_{hn}$ is the specific heat of the hybrid nanofluid and C_p is the specific heat of nanoparticles in J/kg.K.

4.5.4 The viscosity

The viscosity of the HNF is computed according to Batchelor's formula (Murshed et al., 2008) as follows:

$$\mu_{hn} = \frac{\mu_f}{\left[1 - (\emptyset_{\mathrm{SiO2}} + \emptyset_{\mathrm{TiO2}})\right]^{2.5}}, \tag{19}$$

4.6 Economic and exergoeconomic assessment

To accomplish the cost study of the distillation system without and with HNF, several parameters were considered, such as the initial cost of the solar still system (Ps), maintenance cost per year (AMC), salvage value per year (ASV), and the interest rate (i) was supposed to be equal 10%. The initial parameter in the cost analysis is the Capital recovery factor (CRF) which can be defined as (Gad et al., 2022):

$$CRF = \frac{i(1 + i)^n}{(1 + i)^n - 1} \tag{20}$$

Then, the total operational cost of the distillation system (UAC) per year is estimated by (Gad et al. 2022; Yousef et al., 2022):

$$UAC = FAC + AMC - ASV, \tag{21}$$

where FAC is the fixed yearly cost that is calculated as the following:

$$FAC = CRF \times P_s, \tag{22}$$

and AMC is the maintenance cost per year, which is assumed to be 15% of the AMC:

$$AMC = 0.15 \times FAC \tag{23}$$

The salvage value (S) of the solar still system is an important parameter and is considered by (Refat et al. 2019):

$$S = 0.2 \times P_s \tag{24}$$

SFF and ASV can be assessed according to the subsequent formulations, respectively (Refat et al., 2019):

$$SSF = \frac{i}{(1+i)^n - 1}, \tag{25}$$

$$ASV = SSF \times S. \tag{26}$$

Finally, the price per litre for the solar still system can be computed by (Gad et al. 2022; Yousef et al., 2022):

$$\mathrm{CPL} = \frac{UAC}{P_n}. \tag{27}$$

where P_n is the average annual of the produced water from the distillation system.

Due to the importance of the exergy analysis, which considers the real magnitude of thermodynamics and presents an actual measure of the system performance. So, in the current study, the exergoeconomic parameter (R_{exe}) for all the suggested desalination systems can be assessed by the following relation:

$$R_{exe} = \frac{E_{X_{out}}}{UAC}$$

4.7 Environmental and enviroeconomic evaluation

An environmental calculation had to be accomplished by computing the amount of CO_2 realized to the ambient to display the ecological and sustainability result of the MSS on the environment in addition to measuring its environmental superiority alongside the other traditional sources of energy. Therefore, the annual quantity of CO_2 mitigated in tons from the SS systems is set as (Yousef et al., 2022):

$$\emptyset_{co_2} = \frac{2\left(E_{n_{out}} \times n\right)}{1000} \tag{28}$$

where $\emptyset_{co_2}$ is the parameter of environmental and E_n is the energy output from the solar still systems throughout the year. The enviroeconomic analysis is estimated as (Yousef et al., 2022):

$$Z_{co_2} = \emptyset_{co_2} \times z_{co_2} \tag{29}$$

where Z_{co_2} is the parameter of enviro-economic and z_{co_2} is the cost of carbon. The price was expected to be 14.5 \$/ton.

5 Numerical solution

In this section, a numerical solution for computing the hourly changes in temperatures for the SS system by Atangana-Baleanu (AB) fractional operator is studied.

To rewrite the model given by Eqs. (4–8) in the sense of the Atangana-Baleanu fractional derivative, we need to replace the classical derivatives in the equations with Atangana-Baleanu fractional derivatives, then we have:

$${}_0^{AB}\mathbb{D}_t^{\alpha} T = F(T), \quad T(0) = T_0\ , 0 < \alpha < 1 \tag{30}$$

$${}_0^{AB}\mathbb{D}_t^{\alpha}\boldsymbol{T} = \begin{pmatrix} {}_0^{AB}\mathbb{D}_t^{\alpha} T_{gl} \\ {}_0^{AB}\mathbb{D}_t^{\alpha} T_{wat} \\ {}_0^{AB}\mathbb{D}_t^{\alpha} T_{ab} \end{pmatrix}, \boldsymbol{T} = \begin{pmatrix} T_{gl} \\ T_{wat} \\ T_{ab} \end{pmatrix}, \boldsymbol{T}_0 = \boldsymbol{T_{amb}}, F(\boldsymbol{T}) = \begin{pmatrix} f_1\left(t, T_{gl}, T_{wat}, T_{ab}\right) \\ f_2\left(t, T_{gl}, T_{wat}, T_{ab}\right) \\ f_3\left(t, T_{gl}, T_{wat}, T_{ab}\right) \end{pmatrix},$$

where

$$\begin{aligned} f_1\left(t, T_{gl}, T_{wat}, T_{ab}\right) &= \omega_1 T_{wat} - g_1 T_{gl} + s_1 T_{sky} + a_1 T_{amb} + G_1(t), \\ f_2\left(t, T_{gl}, T_{wat}, T_{ab}\right) &= -\omega_2 T_w at + g_2 T_{gl} + p_1 T_{ab} + G_2(t), \\ f_3\left(t, T_{gl}, T_{wat}, T_{ab}\right) &= -\omega_3 T_{wat} + p_2 T_{ab} + a_2 T_{amb} + G_3(t), \end{aligned}$$

and

$$\begin{aligned} &\omega_1 = \frac{h_2 A_{wat}}{m_{gl} c_{gl}},\ g_1 = \frac{1}{m_{gl} c_{gl}}\left(h_2 A_{wat} + h_{cgl-a} A_{gl} + h_{rgl-s} A_{gl}\right), \\ &s_1 = \frac{h_{rgl-s} A_{gl}}{m_{gl} c_{gl}}, a_1 = \frac{h_{cgl-a} A_{gl}}{m_{gl} c_{gl}}, G_1(t) = \frac{\alpha_{\text{eff},gl} A_{gl}}{m_{gl} c_{gl}} G(t), \\ &\omega_2 = \frac{1}{m_{wat} c_{wat}}\left(h_1 A_{ab} + h_2 A_{wat}\right), g_2 = \frac{h_2 A_{wat}}{m_{wat} c_{wat}}, p_1 = \frac{h_1 A_{ab}}{m_{wat} c_{wat}},\ G_2(t) = \frac{\alpha_{\text{eff},wat} A_{wat}}{m_{wat} c_{wat}} G(t), \\ &\omega_3 = \frac{1}{m_{ab} c_{ab}}\left(h_1 A_{ab}\right), p_2 = \frac{1}{m_{ab} c_{ab}}\left(h_1 A_{ab} - H_b A_{ab}\right), a_2 = \frac{1}{m_{ab} c_{ab}}\left(H_b A_{ab}\right), G_3(t) = \frac{\alpha_{\text{eff},ab} A_{ab}}{m_{ab} c_{ab}} G(t). \end{aligned}$$

Now, using the following approximation (Atangana & Baleanu, 2016), the previous equation will be written as follows:

$$\boldsymbol{T}_{n+1} = \boldsymbol{T}_n + w_1(n,\alpha,\Delta t)F(\boldsymbol{T}(t_n)) + w_2(n,\alpha,\Delta t)F(\boldsymbol{T}(t_{n-1})). \tag{31}$$

Use the above approximation. We get the following numerical scheme:

$$\begin{aligned}
T_{gl,n+1} &= T_{gl,n} + w_1(n,\alpha,\Delta t)f_1(t_n, T_{gl,n}, T_{wat,n}, T_{ab,n}) + w_2(n,\alpha,\Delta t)f_1(t_{n-1}, T_{gl,n-1}, T_{wat,n-1}, T_{ab,n-1}),\\
T_{wat,n+1} &= T_{wat,n} + w_1(n,\alpha,\Delta t)f_2(t_n, T_{gl,n}, T_{wat,n}, T_{ab,n}) + w_2(n,\alpha,\Delta t)f_2(t_{n-1}, T_{gl,n-1}, T_{wat,n-1}, T_{ab,n-1}),\\
T_{ab,n+1} &= T_{ab,n} + w_1(n,\alpha,\Delta t)f_3(t_n, T_{gl,n}, T_{wat,n}, T_{ab,n}) + w_2(n,\alpha,\Delta t)f_3(t_{n-1}, T_{gl,n-1}, T_{wat,n-1}, T_{ab,n-1}),
\end{aligned}$$

where $w_1(n,\alpha,\Delta t) = \left[\frac{1-\alpha}{M(\alpha)} - \frac{\alpha}{M(\alpha)\Gamma(\alpha)}(\Delta t)^\alpha\left(\frac{2(n+1)^\alpha}{\alpha} - \frac{(n+1)^{\alpha+1}}{\alpha+1}\right) - \frac{\alpha}{M(\alpha)\Gamma(\alpha)}(\Delta t)^\alpha\left(\frac{n^\alpha}{\alpha} - \frac{n^{\alpha+1}}{\alpha+1}\right)\right]$,

$$w_2(n,\alpha,\Delta t) = \left[\frac{\alpha-1}{M(\alpha)} - \frac{\alpha}{M(\alpha)} - \frac{\alpha}{M(\alpha)\Gamma(\alpha)}(\Delta t)^\alpha\left(\frac{(n+1)^\alpha}{\alpha} - \frac{(n+1)^{\alpha+1}}{\alpha+1} + \frac{n^{\alpha+1}}{M(\alpha)\Gamma(\alpha)\Delta t}\right)\right],$$

and $M(\alpha)$ is the Atangana-Baleanu function, where $M(0) = M(1) = 1$. Δt is the time step.

6 Results and discussions

The results and discussion system are divided into two subsections: model validation and the influence of hybrid nanofluid on SS output.

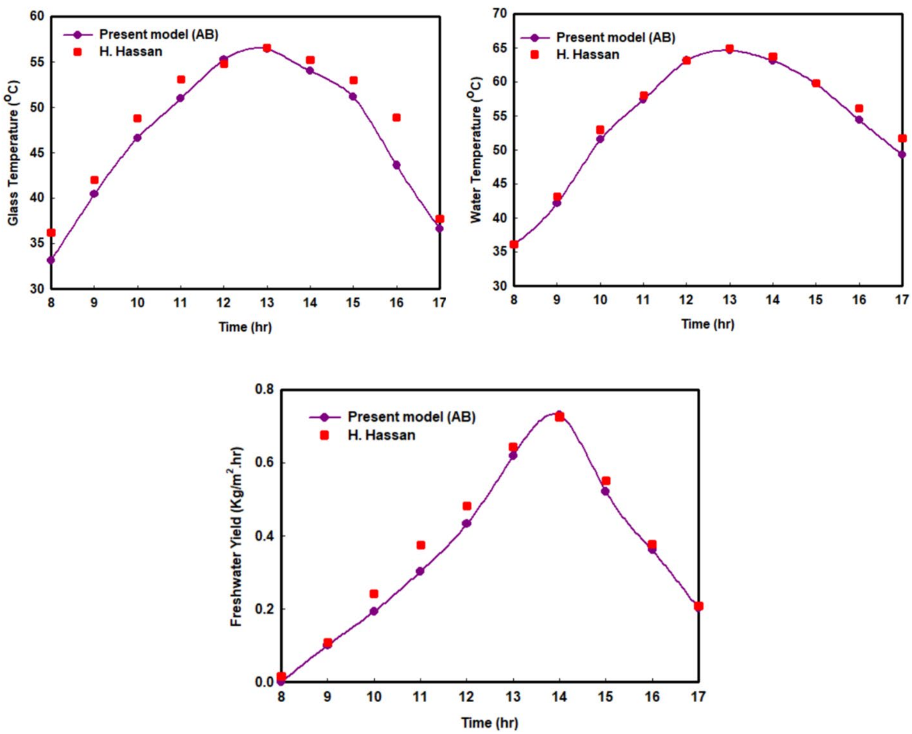

Fig. 2 Variation of the solar still temperature and water productivity for the present model and Hassan (2020) experimental results

Table 1 The optical and thermal properties of the proposed hybrid nanofluid

Nanoparticle category	The Density (kg/m^3)	The Thermal conductivity (W/m K)	The Specific heat (J/kg K)
SiO_2	2270	1.4	745
TiO_2	4250	8.9	692

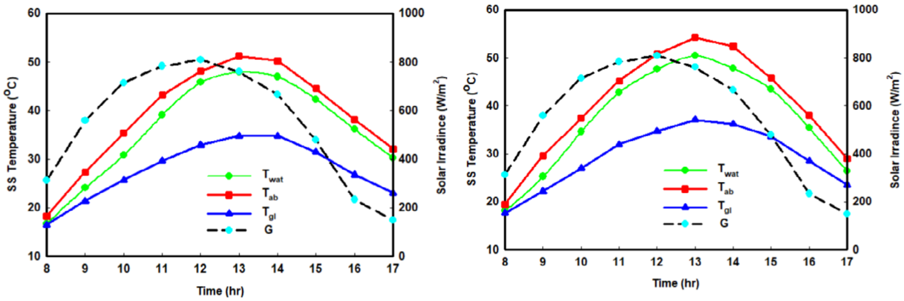

(a) Without HNF (b) With HNF

Fig. 3 Hourly change in SS temperatures in cold climate conditions

6.1 Model validation

Figure 2a–c displays a comparison between the hourly trends in glass temperature, freshwater production, and brackish water temperature in the SS basin using the experimental data from Hassan (2020) and the newly proposed fractional model. Based on the graph, the hourly variation in SS temperatures and SS freshwater production using the AB operator exhibits a remarkable consistency with the actual experimental data. The reason lies in the fact that the non-locality and non-singularity of kernel features, along with a noble memory influence, are considered by the fractional operator. The proposed fractional model simulates the SS behaviour effectively, with a percent of relative error for the greatest values of temperature of the glass, briny water temperature, and freshwater yield being 0.202%, 0.539%, and 0.757%, respectively.

6.2 Influence of using hybrid nanoparticles

The CSS suffers from lower productivity and inadequate thermal performance primarily due to radiative and convective heat losses. However, the utilization of nanofluids has emerged as a promising technique to address these limitations. Nanofluids, created by incorporating nanometre-sized additives into a base fluid, exhibit superior thermophysical and optical properties, enabling enhanced heat transfer and decreased heat loss, resulting in increased freshwater production. By employing nanofluids, heat transfer coefficients are elevated, leading to improved performance of solar stills. Hybrid nanofluids, in particular, offer superior heat transfer capabilities in thermal processes, showcasing enhanced thermophysical properties compared to both conventional fluids and mono nanofluids. This research suggests a mixture of SiO_2 and TiO_2 nanoparticles, each at a volume fraction

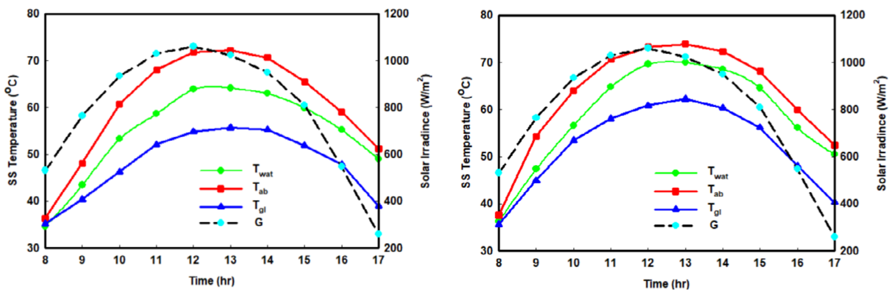

(a) Without HNF (b) With HNF

Fig. 4 Hourly change in SS temperatures in hot climate conditions

percentage of 0.025%, to be added to saline water. The scientific properties of these nanoparticles are explained in Table 1.

6.2.1 Influence on Temperatures

The evaporation of salted water and the subsequent production of freshwater in the SS system is positively influenced by boosting the temperature of the briny water. Figure 3a, b provide a comparison of the hourly variations of the distilled system temperatures during the winter season, both with and without the utilization of hybrid nanofluids. Similarly, Fig. 4a, b display the same temperature results but for the summer period. These figures also include the atmosphere temperature and incident solar radiation during the measurement periods. Upon examining Figs. 3 and 4, it is evident that the behaviour of the SS temperatures remains consistent when hybrid nanofluids are employed, resembling the case of using normal saline water fluid. Notably, a comparison of the water temperatures reveals that the presence of hybrid nanofluids leads to higher water temperatures, particularly during the summer season.

The observed temperature increase can be attributed to the introduction of nanoparticles into the briny water, which enhances the thermophysical properties of the base fluid and consequently improves heat transfer, particularly in warm weather conditions,

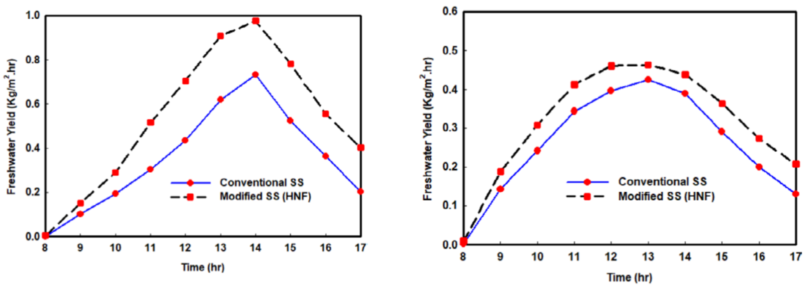

(a) Summer (b) Winter

Fig. 5 Variations of freshwater yield with and without hybrid nano

Table 2 Average water productivity per day in both hot and cold climate conditions

Average water productivity (kg/m^2.day)	Conventional solar still (Without HNF)	Modified solar still (With HNF)
Hot climate conditions	3.4661	5.2922
Cold climate conditions	2.5620	3.1295

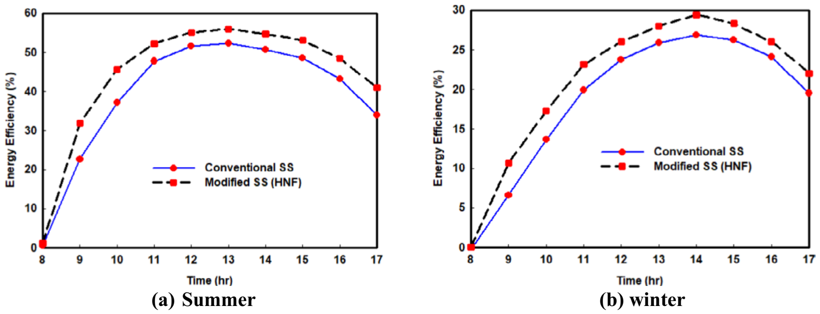

Fig. 6 Variations of SS energy efficiency without and with hybrid nano

resulting in elevated temperature readings. For example, without the inclusion of hybrid nanoparticles, the maximum water temperatures in winter and summer peak at 47.91 °C and 64.15 °C, respectively. However, with the incorporation of hybrid nanofluids, these temperatures escalate to 50.42 °C and 69.99 °C, respectively, representing a noteworthy increase of 5.23% and 9.1% during the winter and summer seasons, respectively. Moreover, in hot climatic conditions, the peak glass temperature at midday rises from 55.73°C to 62.27°C following the introduction of the hybrid nanofluid, indicating a rise of 6.54°C in hot conditions.

6.2.2 Influence on productivity

The primary objective of the solar still (SS) system is to generate freshwater from saline water by harnessing solar radiation. Figure 5a, b depict the hourly variations in freshwater productivity during winter and summer, both with and without the incorporation of hybrid nanofluids. It is evident from Fig. 5 that the amount of freshwater is higher in summer compared to winter, attributed to the greater solar insolation and, consequently, higher water temperature during the summer season, as previously explained. Furthermore, the use of hybrid nanoparticles leads to increased productivity in the solar still system as opposed to using only briny water. The maximum hourly values of freshwater production in winter and summer are 0.4253 kg/m^2 and 0.7317 kg/m^2, respectively, for the system utilizing only saline water, while they reach 0.464 kg/m^2 h and 0.9772 kg/m^2 h, respectively, for the system incorporating hybrid nanoparticles.

The observed enhancement in freshwater yield can be ascribed to the improved rates of condensation and evaporation of briny water facilitated by the application of hybrid nanofluids. Detailed results are presented in Table 2, illustrating the average daily freshwater yield for the solar still system both without and with hybrid nanoparticles. During summer, the daily productivity with hybrid nanoparticles reaches 5.2922 kg/m^2·day, reflecting

Table 3 Average energy efficiency per day in both hot and cold climate conditions

Average Energy Efficiency	Desalination system (Without HNF) (%)	Desalination system (With HNF) (%)
Hot climate conditions	38.84	43.95
Cold climate conditions	18.63	21.10

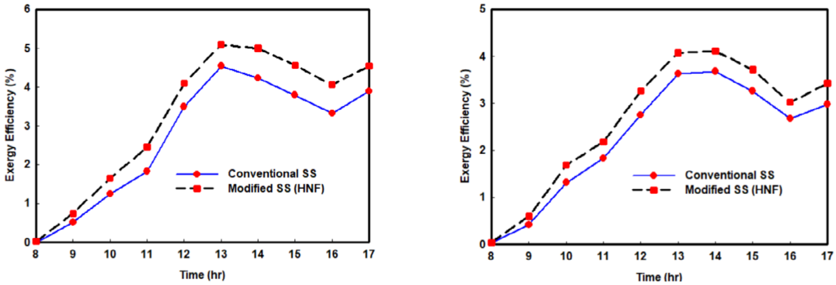

Fig. 7 Variations of SS exergy efficiency with and without hybrid nano

a notable increase of 27.2% compared to the still without nanoparticles. In winter, there is a commendable productivity increase of 21.7%, resulting in a daily yield of 3.1295 kg/ m^2·day. Importantly, the amplified freshwater production due to nanoparticle usage is more prominent in summer, aligning with the heightened solar energy availability during that season. This amplification is consistent with the augmented impact of heat transfer enhancement with saline water through nanoparticle utilization, as elucidated in earlier discussions.

6.2.3 Influence on energy efficiency

During this analysis, we analyzed the energy efficiency of SS without and with HNF, both in winter and summer. Figure 6a, b depict the varying energy efficiency over time, with results showing an increase in energy efficiency from 8 a.m. to close 2 p.m. followed by a gradual decline, similar to the productivity curve. As expected, solar efficiency was still lower in winter than in summer. Furthermore, the use of hybrid nanofluid had a substantial effect on the SS's efficiency, as it increased still productivity, ultimately resulting in higher energy efficiency.

Results showed that the maximum energy efficiency with and without HNF in summer was 56.06% and 52.25%, respectively, while in winter, it was 29.45% and 26.9%, respectively. This represents an increase of 7.3% and 9.4% in summer and winter, respectively. In Table 3, we present the average energy efficiency for the distilled system per day without and with HNF in winter and summer. The results demonstrate that in summer, the average efficiency increased by 13.1% when hybrid nano was used, achieving a maximum average efficiency of 43.95%. In comparison, the increase in efficiency in winter was 11.85%. The findings emphasize the potential of using hybrid nanofluid to enhance solar still efficiency.

Table 4 Average exergy efficiency per day in both hot and cold climate conditions

Average Exergy Efficiency	Conventional solar still (Without hybrid nano) (%)	Modified solar Still (With hybrid nano) (%)
Hot climate conditions	2.68	3.22
Cold climate conditions	2.25	2.61

6.2.4 Influence on exergy efficiency

This section delves into the influence of hybrid nanoparticles on exergy efficiency, a crucial aspect in engineering and thermodynamics for assessing and optimizing energy systems. Unlike traditional energy analysis focusing solely on energy quantity, exergy analysis studies both the quantity and property of energy, making it a powerful tool. Figure 7a, b illustrate hourly fluctuations of exergy efficiency during summer and winter, respectively, comparing scenarios without and with hybrid nanoparticles. It's evident that exergy efficiency peaks around 1 p.m. and gradually declines. Notably, exergy efficiency tends to be lower than energy efficiency due to accounting for system irreversibilities and losses. Employing hybrid nanoparticles leads to higher exergy efficiency, with a more pronounced impact in summer due to increased solar energy availability. Peak exergy efficiency in summer rises from approximately 4.54% to nearly 5.09% with nanoparticle integration, while in winter, values increase from 3.68% to 4.11%. Table 4 presents average exergy efficiency per day, revealing a notable enhancement of approximately 20.14% in summer and 16.4% in winter with hybrid nanoparticles. This improvement stems from increased freshwater productivity facilitated by hybrid nanofluids, as previously demonstrated.

6.3 Cost analysis for n = 10, i = 12%

The economic analysis, presented in Sect. 6.3 for n = 10 and i = 12%, meticulously evaluates the cost per litre (CPL) over a ten-year lifespan for the proposed SS systems during both winter and summer. Table 5 gives a detailed breakdown of the economic assessment. Notably, the incorporation of hybrid nanofluid in the modified solar still demonstrates a substantial reduction in CPL values compared to the CSS in both seasons. During summers, the CPL value for the modified SS with HNF is remarkably low at 0.0156 $/L, presenting a significant cost decrease of over 44% compared to the conventional still (0.0225 $/L). This reduction in CPL is attributed to the considerable enhancement in annual freshwater productivity resulting from the integration of hybrid nanofluid. The observed seasonal variation in CPL, with lower values during summer than winter, is primarily influenced by more favorable weather conditions and increased freshwater productivity in the former season.

Table 5 The cost analysis for all the proposed SS systems without and with HNF

	System	P ($)	CRF	FAC ($)	S	SSF	ASV ($)	AMC ($)	UAC ($)	P_n	CPL ($/L)
Summer	CSS	188	0.1769	33.27	37.6	0.4748	17.85	3.327	18.747	831.86	0.0225
	MSS	199.2	0.1769	35.25	39.84	0.4748	18.91	3.525	19.865	1270.12	0.0156
Winter	CSS	188	0.1769	33.27	37.6	0.4748	17.85	3.327	18.747	614.88	0.0304
	MSS	199.2	0.1769	35.25	39.84	0.4748	18.91	3.525	19.865	750.96	0.0264

Table 6 Parameters of Exergoeconomic for all proposed systems

	System	*n*	*i*	UAC ($)	E_{xout} (kWh) Annual	R_{exe} (kWh/$)
Summer	CSS	10	12	18.747	83.985	4.47
	MSS	10	12	19.865	131.21	6.605
Winter	CSS	10	12	18.747	64.325	3.43
	MSS	10	12	19.865	78.48	3.95

6.4 Calculations of exergoeconomic parameters for n = 10, i = 12%

Exergoeconomic analysis plays a vital role in assessing the total efficiency and economic viability of energy systems. By combining the principles of thermodynamics and economics, engineers and policymakers enable to prioritize energy optimization strategies and make informed decisions regarding energy investments. The tabular representation of the calculation of R_{exe} for both the MCC and CSS systems across various seasons, i.e., summer and winter, is depicted in Table 6. On keenly observing the table, it becomes apparent that the MCC system, which utilizes a hybrid nanofluid, outperforms the CSS system in terms of R_{exe} for both summer and winter. As an example, the R_{ex} for the MCC and CSS systems in summer is calculated to be 6.605 (kWh/$) and 4.47 (kWh/$), respectively. This variance in R_{exe} indicates that the former system outperforms the latter by approximately 47.7%. This improvement in R_{exe} can be attributed to a minor increase in the UAC of the MCC system. However, its significant effect on the annual exergy output surpasses the decrease in UAC, resulting in a higher exergoeconomic parameter. Nonetheless, during winters, this increase of R_{exe} with respect to the MSS system witnesses a slight reduction of 15.1%, as opposed to summers, due to a decrease in freshwater production enhancements.

6.5 Environmental and enviroeconomic analysis

Environmental and enviroeconomic analyses are of paramount importance when it comes to an understanding and mitigating CO_2 emissions, which are a major contributor

Table 7 Environmental analysis for all the proposed solar still systems with and without HNF

Parameters	Summer		Winter	
	CSS	MSS	CSS	MSS
En_{out} (kWh) annual	819.32	923.61	572.5	742.22
Ex_{out} (kWh) annual	83.985	131.21	64.325	78.48
En_{out} (kWh) for lifetime	8193.2	9236.1	5725	7422.2
Ex_{out} (kWh) for lifetime	839.85	1312.1	643.25	784.8
Parameter of Environmental (Rate ton Co_2/year)	16.38	18.47	11.45	14.84
Enviroeconomic parameter (Rate $/year)	237.6	267.84	166.025	215.24
Parameter of Exergoenvironmental Rate ton Co_2/year	1.6797	2.6242	1.28651	1.5696
Parameter of Exergoenviroeconomic (Rate $/year)	24.355	38.05	18.654	22.7592

to climate change. The environmental analysis focuses on assessing the mitigating CO_2 emissions. Enviroeconomic analysis, on the other hand, combines environmental factors with economic considerations to evaluate the costs and benefits associated with reducing CO_2 emissions. This analysis aids policymakers, businesses, and individuals in making informed decisions by highlighting the environmental and economic trade-offs and identifying the most effective and economically viable pathways to reduce CO_2 emissions. Table 7 provides a comparative overview of summer and winter environmental and enviro-economic evaluations conducted using energy and exergy methodologies. In terms of the environmental approach, the findings indicate that during summer, CSS and MSS mitigated 16.38 and 18.47 tons of CO_2/year, respectively.

The exergy-environmental approach, on the other hand, found these values to be 1.68 and 2.62 tons CO_2/year, respectively. These results reveal that MSS mitigated about 12.7% more CO_2 mitigation during summer when compared with CSS based on energy approaches. This trend is owing to the higher energy generated by MSS than the embodied energy integration of hybrid Nanofluid, resulting in increased CO_2 mitigation. Similarly, the findings based on the exergy approach suggest that MSS mitigated approximately 56.2% more CO_2 compared to CSS. Wintertime results show that compared to CSS, MSS mitigated approximately 29.6% and 22% more CO_2 based on energy and exergy approaches, respectively. Additionally, it is noteworthy that the addition of hybrid nanofluid to solar still significantly improved the enviro-economic parameter, as highlighted in Table 7. In summer, the enviro-economic parameter for CSS and MSS was 237.6$ and 267.84$, respectively, According to the energy approach. The exergy-environmental approach produced equivalent values of 24.355$ and 38.05$, respectively.

7 Conclusion

The influence of titanium oxide (TiO_2) and silicon oxide (SiO_2) hybrid nanoparticles on the solar still performance (SS) is studied by applying a new numerical method based on the Atangana- Baleanu (AB) fractional operator. In addition, a comparison is conducted between the numerical findings of a fractional model and experimental data for the climate of Upper Egypt. The findings indicate that a fractional model corresponds to the actual experiment. It indicates that the error percentage in the extreme value of freshwater yield reaches approximately 0.757%. According to the fractional approach, the results demonstrate that the addition of hybrid nanoparticles to the solar still has a substantial influence on it in terms of boosting the quantity of freshwater production and enhancing both exergy and energy efficiency, with the winter impact being less pronounced than the summer impact. It has been shown that utilizing hybrid nanoparticles with the saltwater of CSS increases the production by approximately 27.2% in Summer and 21.7% in Winter. Additionally, its average daily efficiency increases to approximately 21.1% and 43.95% in winter and summer, respectively. In cold and hot climates, the average exergy efficiency of the SS per day is increased by 16.4% and 20.14%, respectively, when nanoparticles are added to saline water. An economic investigation showed that in the summer, SS with hybrid nanofluid reported a cost-per-liter reduction of over 44% compared to CSS. In terms of enviroeconomic analysis, findings indicate that SS with nanofluid mitigated approximately 12.7% more CO_2 during the summer than CSS based on energy approaches. Whereas, Wintertime results indicate that SS with nanofluid mitigated nearly 29.6% and 22% more CO_2 than CSS using energy and exergy approaches, respectively. For the future work, the effect of using HNF in active and passive SS should be investigated.

Our study has significant implications for key stakeholders. Policymakers can leverage hybrid nanofluids to improve solar still performance and promote sustainable freshwater production through supportive policies and funding. Academics can advance research in solar energy and nanofluid applications using our novel fractional model. Additionally, our findings offer valuable insights for researchers and businesses in renewable energy, highlighting the economic and environmental benefits of integrating hybrid nanofluids into solar still systems and suggesting avenues for commercialization and scale-up efforts.

Acknowledgements The authors are pleased to acknowledge Benha University for supporting the present work.

Funding Open access funding provided by The Science, Technology & Innovation Funding Authority (STDF) in cooperation with The Egyptian Knowledge Bank (EKB).

Declarations

Conflicts of interest The authors declare no competing interests.

References

Abd Elbar, A. R., Yousef, M. S., & Hassan, H. (2019). Energy, exergy, exergoeconomic and enviroeconomic (4E) evaluation of a new integration of solar still with photovoltaic panel. *Journal of Cleaner Production, 233*, 665–680. https://doi.org/10.1016/j.jclepro.2019.06.111

Abdullah, A. S., Alawee, W. H., Mohammed, S. A., Majdi, A., Omara, Z. M., & Younes, M. M. (2023). Utilizing a single slope solar still with copper heating coil, external condenser, phase change material, along with internal and external reflectors—experimental study. *Journal of Energy Storage, 63*, 106899. https://doi.org/10.1016/j.est.2023.106899

Abo-Elfadl, S., Yousef, M. S., & Hassan, H. (2021). Energy, exergy, and enviroeconomic assessment of double and single pass solar air heaters having a new design absorber. *Process Safety and Environmental Protection, 149*, 451–464. https://doi.org/10.1016/j.psep.2020.11.020

Abujazar, M. S. S., Fatihah, S., Rakmi, A. R., & Shahrom, M. Z. (2016). The effects of design parameters on productivity performance of a solar still for seawater desalination: A review. *Desalination, 385*, 178–193. https://doi.org/10.1016/j.desal.2016.02.025

Ahmed, M. M., Alshammari, F., Alqsair, U. F., Alhadri, M., Abdullah, A. S., & Elashmawy, M. (2022). Experimental study on the effect of the black wick on tubular solar still performance. *Case Studies in Thermal Engineering, 38*, 102333. https://doi.org/10.1016/j.csite.2022.102333

Ajit, G. K., Malik, P., Garg, H., & Lamba, R. (2023). Thermophysical properties analysis of Al_2O_3, MgO and GO nanofluids with water for solar still. *Materials Today: Proceedings*. https://doi.org/10.1016/j.matpr.2023.06.383

Alsehli, M. (2022). Application of graphene nanoplatelet/platinum hybrid nanofluid in a novel design of solar still for improving water production and energy management. *Sustainable Energy Technologies and Assessments, 53*, 102607. https://doi.org/10.1016/j.seta.2022.102607

Alshqirate, A., Awad, A. S., Al Alawin, A., & Essa, M. A. (2023). Experimental investigation of solar still productivity enhancement of distilled water by using natural fibers. *Desalination, 553*, 116487. https://doi.org/10.1016/j.desal.2023.116487

Aly, W. I., Tolba, M. A., & Abdelmagied, M. (2023). Experimental investigation and performance evaluation of an oval tubular solar still with phase change material. *Applied Thermal Engineering, 221*, 119628. https://doi.org/10.1016/j.applthermaleng.2022.119628

Aminossadati, S. M., & Ghasemi, B. (2009). Natural convection cooling of a localised heat source at the bottom of a nanofluid-filled enclosure. *European Journal of Mechanics - B/Fluids, 28*, 630–640.

Angappan, G., Pandiaraj, S., Alrubaie, A. J., Muthusamy, S., Said, Z., Panchal, H., & Kabeel, A. E. (2023). Investigation on solar still with integration of solar cooker to enhance productivity: Experimental, exergy, and economic analysis. *Journal of Water Process Engineering, 51*, 103470. https://doi.org/10.1016/j.jwpe.2022.103470

Asbik, M., Ansari, O., Bah, A., Zari, N., Mimet, A., & El-Ghetany, H. (2016). Exergy analysis of solar desalination still combined with heat storage system using phase change material (PCM). *Desalination, 381*, 26–37. https://doi.org/10.1016/j.desal.2015.11.031

Atangana, A., & Baleanu, D. (2016). New fractional derivatives with nonlocal and non-singular kernel: Theory and application to heat transfer model. *Thermal Science, 4*, 763–769.

Bait, O., & Si-Ameur, M. (2018). Enhanced heat and mass transfer in solar stills using nanofluids: A review. *Solar Energy, 170*, 694–722. https://doi.org/10.1016/j.solener.2018.06.020

Bourantas, G. C., & Loukopoulos, V. C. (2014). Modeling the natural convective flow of micropolar nanofluids. *International Journal of Heat and Mass Transfer, 68*, 35–41.

Chauhan, V. K., & Shukla, S. K. (2023). Performance analysis of prism shaped solar still using black phosphorus quantum dot material and lauric acid in composite climate: An experimental investigation. *Solar Energy, 253*, 85–99. https://doi.org/10.1016/j.solener.2023.02.017

Chen, W., Zhou, J., Zhang, F., Li, X., & Guo, J. (2023). Stability study of low-cost carbon quantum dots nanofluids with saline water and their application investigation for the performance improvement of solar still. *Diamond and Related Materials, 138*, 110194. https://doi.org/10.1016/j.diamond.2023.110194

Deniz, E., & Çınar, S. (2016). Energy, exergy, economic and environmental (4E) analysis of a solar desalination system with humidification-dehumidification. *Energy Conversion and Management, 126*, 12–19. https://doi.org/10.1016/j.enconman.2016.07.064

Elbar, A., & Hassan, H. (2019). An experimental work on the performance of solar still incorporating with wind turbine and thermal energy storage unit. *Desalination Water Treat, 165*, 24–34. https://doi.org/10.5004/dwt.2019.24492

Elbar, A. R. A., Yousef, M. S., & Hassan, H. (2019). Energy, exergy, exergoeconomic and enviroeconomic (4E) evaluation of a new integration of solar still with photovoltaic panel. *Journal of Cleaner Production, 233*, 665–680. https://doi.org/10.1016/j.jclepro.2019.06.111

El-Gazar, E. F., Hassan, H., Rabia, S. I., & Zahra, W. K., (2023a). The thermal performance of the photovoltaic panel under the effect of air and water cooling: Modeling and simulation. In *International Conference of Numerical Analysis and Applied Mathematics Icnaam 2021.*

El-Gazar, E. F., Hassan, H., Rabia, S. I., Hu, C., & Zahra, W. K. (2023b). A new fractional Cattaneo model for enhancing the thermal performance of photovoltaic panels using heat spreader: Energy, exergy, economic and enviroeconomic (4E) analysis. *Environmental Science and Pollution Research, 30*(48), 105840–105855. https://doi.org/10.1007/s11356-023-29654-8

El-Gazar, E. F., Hassan, H., Rabia, S. I., & Zahra, W. K. (2021a). Study of the impact of using hybrid nanofluid and saline water preheating on the performance of both integrated solar still and photovoltaic panel using fractional modeling. *The European Physical Journal Plus, 136*, 1–37. https://doi.org/10.1140/epjp/s13360-021-01654-y

El-Gazar, E. F., Zahra, W. K., Hassan, H., & Rabia, S. I. (2021b). Fractional modeling for enhancing the thermal performance of conventional solar still using hybrid nanofluid: Energy and exergy analysis. *Desalination, 503*, 114847. https://doi.org/10.1016/j.desal.2020.114847

Gad, R., Mahmoud, H., Ookawara, S., & Hassan, H. (2022). Energy, exergy, and economic assessment of thermal regulation of PV panel using hybrid heat pipe-phase change material cooling system. *Journal of Cleaner Production, 364*, 132489. https://doi.org/10.1016/j.jclepro.2022.132489

Gaur, A., & Tiwari, G. N. (2014). Exergoeconomic and enviroeconomic analysis of photovoltaic modules of different solar cells. *Journal of Solar Energy, 2014*, 1–8. https://doi.org/10.1155/2014/719424

Gupta, A., Gupta, A., Yadav, A. C., & Kumar, A. (2022). Performance analysis of single slope solar still under composite climate in India: Numerical simulation and thermal modeling approach. *Materials Today: Proceedings, 63*, 699–705. https://doi.org/10.1016/j.matpr.2022.04.956

Hakim, A. R., Handoyo, W. T., & Wullandari, P. (2018). An energy and exergy analysis of photovoltaic system in Bantul Regency, Indonesia. *Journal of Mechatronics, Electrical Power, and Vehicular Technology, 9*(1), 1–7. https://doi.org/10.14203/j.mev.2018.v9.1-7

Hameed, H. G. (2022). Experimentally evaluating the performance of single slope solar still with glass cover cooling and square cross-section hollow fins. *Case Studies in Thermal Engineering, 40*, 102547. https://doi.org/10.1016/j.csite.2022.102547

Hassan, H. (2014). Heat transfer of Cu-water nanofluid in an enclosure with a heat sink and discrete heat source. *European Journal of Mechanics, B/fluids, 45*, 72–83. https://doi.org/10.1016/j.euromechflu.2013.12.003

Hassan, H. (2020). Comparing the performance of passive and active double and single slope solar stills incorporated with parabolic trough collector via energy, exergy and productivity. *Renewable Energy, 148*, 437–450. https://doi.org/10.1016/j.renene.2019.10.050

Hassan, H., Ahmed, M. S., Fathy, M., & Yousef, M. S. (2019). Impact of salty water medium and condenser on the performance of single acting solar still incorporated with parabolic trough collector. *Desalination, 480*, 2020. https://doi.org/10.1016/j.desal.2020.114324

Hassan, H., & Harmand, S. (2013). 3D transient model of vapour chamber: Effect of nanofluids on its performance. *Applied Thermal Engineering, 51*(1–2), 1191–1201. https://doi.org/10.1016/j.applthermaleng.2012.10.047

Hassan, H., & Osman, O. O. (2022). Novel dynamic simulation model and detailed performance evaluation of single slope solar still: Impact of side walls material. *Solar Energy, 244*, 298–314. https://doi.org/10.1016/j.solener.2022.08.026

Hassan, H., Yousef, M. S., Ahmed, M. S., & Fathy, M. (2020). Energy, exergy, environmental, and economic analysis of natural and forced cooling of solar still with porous media. *Environmental Science and Pollution Research, 27*(30), 38221–38240. https://doi.org/10.1007/s11356-020-09995-4

Hawwash, A. A., Abdel-Rahman, A. K., & Nada, S. A. (2016) Experimental study of alumina nanofluids effects on thermal performance efficiency of flat plate solar collectors. In *5th Annual International Conference on Sustainable Energy and Environmental Sciences (SEES 2016)*, Global Science & technology Forum (GSTF). https://doi.org/10.5176/2251-189X_SEES16.29.

Hawwash, A. A., Mori, S., El Feky, K., & Hassan, H. (2019) Numerical study for open reactor design using salt hydrate. In *IOP Conference Series: Earth and Environmental Science*, Institute of Physics Publishing, https://doi.org/10.1088/1755-1315/322/1/012021.

Hawwash, A. A., Ahamed, M., Nada, S. A., Radwan, A., & Abdel-Rahman, A. K. (2021). Thermal analysis of flat plate solar collector using different nanofluids and nanoparticles percentages. *IEEE Access, 9*, 52053–52066. https://doi.org/10.1109/ACCESS.2021.3060004

Hawwash, A. A., Mori, S., & Hassan, H. (2023). An experimental investigation on the performance of designed closed reactor system on the thermochemical heat storage of magnesium chloride hexahydrate. *Experimental Heat Transfer*. https://doi.org/10.1080/08916152.2023.2240807

Hawwash, A. A., Rahman, A. K. A., Nada, S. A., & Ookawara, S. (2018). Numerical investigation and experimental verification of performance enhancement of flat plate solar collector using nanofluids. *Applied Thermal Engineering, 130*, 363–374. https://doi.org/10.1016/j.applthermaleng.2017.11.027

HM Hussen MM Younes WH Alawee AS Abdullah SA Mohammed T Atteya ZM Faheem Abbas Omara 2023 An experimental comparison study between four different designs of solar stills Case Studies in Thermal Engineering 44 102841 https://doi.org/10.1016/j.csite.2023.102841

Ibrahim, A. G. M., Rashad, A. M., & Dincer, I. (2017). Exergoeconomic analysis for cost optimization of a solar distillation system. *Solar Energy, 151*, 22–32. https://doi.org/10.1016/j.solener.2017.05.020

Jafarkazemi, F., & Ahmadifard, E. (2013). Energetic and exergetic evaluation of flat plate solar collectors. *Renewable Energy, 56*, 55–63. https://doi.org/10.1016/j.renene.2012.10.031

Joshi, P., & Tiwari, G. N. (2018). Energy matrices, exergo-economic and enviro-economic analysis of an active single slope solar still integrated with a heat exchanger: A comparative study. *Desalination, 443*, 85–98. https://doi.org/10.1016/j.desal.2018.05.012

Kabeel, A. E., et al. (2019). Effect of water depth on a novel absorber plate of pyramid solar still coated with TiO_2 nano black paint. *Journal of Cleaner Production, 213*, 185–191. https://doi.org/10.1016/j.jclepro.2018.12.185

Kaviti, A. K., Akkala, S. R., Ali, M. A., Anusha, P., & Sikarwar, V. S. (2023). Performance Improvement of Solar Desalination System Based on CeO2-MWCNT Hybrid Nanofluid. *Sustainability, 15*(5), 4268. https://doi.org/10.3390/su15054268

Keshtkar, M., Eslami, M., & Jafarpur, K. (2020). Effect of design parameters on performance of passive basin solar stills considering instantaneous ambient conditions: A transient CFD modeling. *Solar Energy, 201*, 884–907. https://doi.org/10.1016/j.solener.2020.03.068

Kianifar, A., Heris, S. Z., & Mahian, O. (2012). Exergy and economic analysis of a pyramid-shaped solar water purification system: Active and passive cases. *Energy, 38*(1), 31–36. https://doi.org/10.1016/j.energy.2011.12.046

R Kumar J Chanda AH Elsheikh B Ongar Y Khidolda S PraveenKumar S Hitesh Panchal Shanmugan 2023 Performance improvement of single and double effect solar stills with silver balls/nanofluids for bioactivation: An experimental analysis Solar Energy 259 452 463 https://doi.org/10.1016/j.solener.2023.05.012

Kumar, N. M., Subramaniam, U., Mathew, M., Ajitha, A., & Almakhles, D. J. (2020). Exergy analysis of thin-film solar PV module in ground-mount, floating and submerged installation methods. *Case Studies in Thermal Engineering, 21*, 100686. https://doi.org/10.1016/j.csite.2020.100686

Kumaravel, S., Nagaraj, M., & Bharathiraja, G. (2022). Experimental investigation on the performance analysis of blue metal stones and pebble stones as thermal energy storage materials in single slope solar still. *Mater Today Proc*. https://doi.org/10.1016/j.matpr.2022.11.100

Lisboa, A. A. V., Segurado, R., & Mendes, M. A. A. (2022). Solar still performance for small-scale and low-cost seawater desalination: Model-based analysis and water yield enhancement techniques. *Solar Energy, 238*, 341–362. https://doi.org/10.1016/j.solener.2022.04.007

Maatki, C. (2022). Heat transfer enhancement using CNT-water nanofluids and two stages of seawater supply in the triangular solar still. *Case Studies in Thermal Engineering, 30*, 101753. https://doi.org/10.1016/j.csite.2021.101753

P Manoj Kumar PT Saravanakumar Atul Sarojwal D Rajasekaran Saminathan SJ Harikrishna RA Prasanth Pranav 2023 Experimental investigations on the performance of a single slope solar still with thermal energy storage Materials Today: Proceedings https://doi.org/10.1016/j.matpr.2022.12.221

Mittal, G. (2021). An unsteady CFD modelling of a single slope solar still. *Materials Today: Proceedings, 46*, 10991–10995. https://doi.org/10.1016/j.matpr.2021.02.090

Modi, K. V., & Gamit, A. R. (2022). Investigation on performance of square pyramid solar still using nanofluid and thermal energy storage material: An experimental and theoretical study. *Journal of Cleaner Production, 381*, 135115. https://doi.org/10.1016/j.jclepro.2022.135115

Moustafa, E. B., Hammad, A. H., & Elsheikh, A. H. (2022). A new optimized artificial neural network model to predict thermal efficiency and water yield of tubular solar still. *Case Studies in Thermal Engineering, 30*, 101750. https://doi.org/10.1016/j.csite.2021.101750

Murshed, S. M., Leong, K. C., & Yang, C. (2008). Thermophysical and electrokinetic properties of nanofluids—A critical review. *Applied Thermal Engineering, 28*, 2109–2152.

Mustafa, J., Abdullah, M. M., Husain, S., Alqaed, S., Malekshah, E. H., & Sharifpur, M. (2023). A two-phase analysis of the use of water-aluminum nanofluid in a solar still with a layer of phase change materials. *Eng Anal Bound Elem, 152*, 627–636. https://doi.org/10.1016/j.enganabound.2023.04.030

Obembe, A. D., Hossain, M. E., & Abu-Khamsin, S. A. (2017). Variable-order derivative time fractional diffusion model for heterogeneous porous media. *Journal of Petroleum Science and Engineering, 152*, 391–405. https://doi.org/10.1016/j.petrol.2017.03.015

Pal, P., Dev, R., Singh, D., & Ahsan, A. (2018). Energy matrices, exergoeconomic and enviroeconomic analysis of modified multi–wick basin type double slope solar still. *Desalination, 447*, 55–73. https://doi.org/10.1016/j.desal.2018.09.006

Rabbi, H. M. F., & Sahin, A. Z. (2021). Performance improvement of solar still by using hybrid nanofluids. *Journal of Thermal Analysis and Calorimetry, 143*(2), 1345–1360. https://doi.org/10.1007/s10973-020-10155-6

Ranjan, K. R., Kaushik, S. C., & Panwar, N. L. (2016). Energy and exergy analysis of passive solar distillation systems. *International Journal of Low-Carbon Technologies, 11*(2), 211–221. https://doi.org/10.1093/ijlct/ctt069

Rashidi, S., Bovand, M., Rahbar, N., & Esfahani, J. A. (2018). Steps optimization and productivity enhancement in a nanofluid cascade solar still. *Renewable Energy, 118*, 536–545. https://doi.org/10.1016/j.renene.2017.11.048

Rashidi, S., Esfahani, J. A., & Rashidi, A. (2017). A review on the applications of porous materials in solar energy systems. *Renewable and Sustainable Energy Reviews, 73*, 1198–1210. https://doi.org/10.1016/j.rser.2017.02.028

Refat, A., Elbar, A., Yousef, M. S., & Hassan, H. (2019). of a new integration of solar still with photovoltaic panel. *Journal of Cleaner Production, 233*, 665–680. https://doi.org/10.1016/j.jclepro.2019.06.111

Sahota, L., Arora, S., Singh, H. P., & Sahoo, G. (2020). Thermo-physical characteristics of passive double slope solar still loaded with mwcnts and al2o3-water based nanofluid. *Materials Today: Proceedings, 32*, 344–349. https://doi.org/10.1016/j.matpr.2020.01.600

Sahota, L., & Shyam, G. N. T. (2017). Energy matrices, enviroeconomic and exergoeconomic analysis of passive double slope solar still with water based nanofluids. *Desalination, 409*, 66–79. https://doi.org/10.1016/j.desal.2017.01.012

Sahu, R., & Tiwari, A. C. (2024). Performance enhancement of single slope solar still using nanofluids at different water depth. *Desalination and Water Treatment, 317*, 100046. https://doi.org/10.1016/j.dwt.2024.100046

Sharshir, S. W., Guilong Peng, A. H., Elsheikh, E. M. A., Edreis, M. A., Eltawil, T. A., Kabeel, A. E., Zang, J., & Yang, N. (2018). Energy and exergy analysis of solar stills with micro/nano particles: A comparative study. *Energy Conversion and Management, 177*, 363–375. https://doi.org/10.1016/j.enconman.2018.09.074

Sharshir, S. W., Kandeal, A. W., Algazzar, A. M., Eldesoukey, A., El-Samadony, M. O. A., & Hussien, A. A. (2022). 4-E analysis of pyramid solar still augmented with external condenser, evacuated tubes, nanofluid and ultrasonic foggers: A comprehensive study. *Process Safety and Environmental Protection, 164*, 408–417. https://doi.org/10.1016/j.psep.2022.06.026

Shoeibi, S., Kargarsharifabad, H., Rahbar, N., Ahmadi, G., & Safaei, M. R. (2022). Performance evaluation of a solar still using hybrid nanofluid glass cooling-CFD simulation and environmental analysis. *Sustainable Energy Technologies and Assessments, 49*, 101728. https://doi.org/10.1016/j.seta.2021.101728

Singh, D. B. (2019). Exergo-economic, enviro-economic and productivity analyses of N identical evacuated tubular collectors integrated double slope solar still. *Applied Thermal Engineering, 148*, 96–104. https://doi.org/10.1016/j.applthermaleng.2018.10.127

Singh, D. B., & Tiwari, G. N. (2017). Exergoeconomic, enviroeconomic and productivity analyses of basin type solar stills by incorporating N identical PVT compound parabolic concentrator collectors: A comparative study. *Energy Conversion and Management, 135*, 129–147. https://doi.org/10.1016/j.enconman.2016.12.039

Sun, H., Chang, A., Zhang, Y., & Chen, W. (2019). A review on variable-order fractional differential equations: Mathematical foundations, physical models, numerical methods and applications. *Fract Calc Appl Anal, 22*(1), 27–59. https://doi.org/10.1515/fca-2019-0003

Teodoro, G. S., Machado, J. T., & De Oliveira, E. C. (2019). A review of definitions of fractional derivatives and other operators. *Journal of Computational Physics, 388*, 195–208. https://doi.org/10.1016/j.jcp.2019.03.008

Toosi, S. S. A., Goshayeshi, H. R., Zahmatkesh, I., & Nejati, V. (2023). Experimental assessment of new designed stepped solar still with Fe3O4+ graphene oxide+ paraffin as nanofluid under constant magnetic field. *Journal of Energy Storage, 62*, 106795. https://doi.org/10.1016/j.est.2023.106795

Yang, L., & Jiang, W. (2017). A new thermal conductivity model for nanorod-based nanofluids. *Applied Thermal Engineering, 114*, 287–299.

Yousef, M. S., & Hassan, H. (2019). Energetic and exergetic performance assessment of the inclusion of phase change materials (PCM) in a solar distillation system. *Energy conversion and management, 179*, 349–361. https://doi.org/10.1016/j.enconman.2018.10.078

Yousef, M. S., Hassan, H., Ahmed, M., & Ookawara, S. (2017). Energy and exergy analysis of single slope passive solar still under Egyptian climate conditions. *Energy Procedia, 141*(00), 18–23. https://doi.org/10.1016/j.egypro.2017.11.005

Yousef, M. S., Sharaf, M., & Huzayyin, A. S. (2022). Energy, exergy, economic, and enviroeconomic assessment of a photovoltaic module incorporated with a paraffin-metal foam composite: An experimental study. *Energy, 238*, 121807. https://doi.org/10.1016/j.energy.2021.121807

Žecová, M., & Terpák, J. (2015). Heat conduction modeling by using fractional-order derivatives. *Applied Mathematics and Computation, 257*, 365–373. https://doi.org/10.1016/j.amc.2014.12.136